Terrain-Adaptive Gait for Walking Machines

María A. Jiménez
P. González de Santos
Instituto de Automática Industrial-CSIC
Departamento de Control Automático
C.N. III, La Poveda
28500 Arganda del Rey, Madrid, Spain

Abstract

One of the primary advantages of walking machines is their inherent capacity for moving over different terrains. However, it is important to provide algorithms that modify the gait according to the terrain. Existing articles about terrain-adaptive locomotion are based on intelligent foothold selection, and use periodic and/or aperiodic gaits. This article proposes a strategy to adapt walking robot locomotion to an irregular terrain in real time that is based on the variations of parameters of a periodic gait affecting leg coordination. Its main feature is that it does not require knowledge of footholds. In addition, this adaptive gait control can be incorporated into a system with external stereoceptive sensors to select footholds. As a working example, a particular class of periodic gaits, called wave-crab gaits, are used in a quadruped robot. However, the proposed adaptive-gait method can be used for any other periodic gait and for robots with a greater number of legs. Adaptive-gait control has been implemented in a quadruped robot named RIMHO, demonstrating its ability to move over different terrains. Static stability results from computer simulations and experimentally obtained velocity results are also presented.

1. Introduction

Gaits can be classified into two major groups: periodic and nonperiodic. Periodic gaits are the most simple to implement, and require less computing time. In principle, however, these gaits lack the ability to walk over uneven terrain. Periodic gaits are characterized by the fact that each leg is placed at a fixed position and operates with the same cycle time. Nonperiodic gaits, on the other hand, are appropriate for uneven terrain because they enable the legs to be placed over previously selected footholds; also, leg placing and lifting sequences are determined in accordance with any optimality criterion (for example, maximization of static stability or minimization of temporal margin). Consequently these nonperiodic gaits are a burden on limited on-board computing resources.

Using periodic gaits, different strategies can be employed to obtain a terrain-adaptive walking machine. Hirose (1984) proposed an adaptive-gait-control algorithm that was formalized for a quadruped vehicle, assuming a horizontal terrain with certain regions unsuitable for support (forbidden zones) and constant speed. The algorithm uses a free gait (a nonperiodic gait) but attempts to maintain the wave gait for crab walking (a periodic gait) that is set as a standard gait. Three principles were developed to choose areas for potential footholds so as to avoid deadlock (the situation whereby one leg, which cannot be lifted due to static stability considerations, reaches a kinematic limit). Also, the proposed algorithm preserves the relative foot position of the standard gait, although it does not consider time-sequencing constraints when the foot positions are at a different height.

Kumar and Waldron (1989), on the other hand, proposed a gait-control algorithm for periodic gaits which automatically adapts the gait to the selected footholds for a wide range of speeds. This algorithm was formalized for a periodic gait called the modified wave gait (MWG). Control strategies to obtain the desired velocity based on modifying gait parameters were also described. In some of these, changes in gait are induced by changes in the duty factor (β) or the leg phase (ϕ_i) whereas others only affect the leg stroke (R) or cycle time (T).

Both adaptive-gait-control strategies involve intelligent foothold selection, although it is possible to walk automatically over certain terrains without using sophisticated external perception sensors. Also, these algorithms do not take into consideration the case in which the information from the external perception sensors is relatively untrustworthy, which can occur in a statically unstable situation. Another drawback is that when these are used, one cannot profit from the advantages offered by *blind* machines, i.e.,

The International Journal of Robotics Research,
Vol. 16, No. 3, June 1997, pp. 320–339,

vehicles that do not know the terrain in advance. Also, these gait-control algorithms have been proven by computer simulation, but there are no experimental results available.

In the case of a blind legged robot that walks over a smooth terrain using a periodic gait, it is possible to fix a specific stroke R (xy-coordinates of footholds). Also, the z-coordinate of footholds may be fixed at a given value if the foothold height is unknown. This can generate statically unstable situations. There are two such cases: 1) when a leg finishes its transfer phase before touching the ground, and 2) when a leg contacts the ground before it was theoretically expected to, according to the gait. To avoid these situations, this article proposes a gait-control strategy for a blind walking robot that automatically adapts the gait to an uneven terrain in real time. This strategy is based on periodic gaits, and uses a particular class of gaits, defined for quadruped machines, called the wave-crab gait (Zhang and Song 1990). The main objective is to maintain the periodic gait and, whenever possible, the velocity, because constant speed is one of the conditions for maximum static stability (Song and Waldron 1987). For the same reason, the body of the machine is considered to be level. To perform the adaptive control, gait parameters affecting leg coordination such as stroke and time period (duty factor affects the sequencing of legs) are modified.

Section 2 defines leg trajectory in the support phase for crab straight-line motion, and also discusses features of two types of transfer-phase leg trajectories in order to select the most adequate. The following section describes the type of terrain that will be considered in this article. Section 4 describes methods of controlling gait parameters to adapt the gait to the terrain. A strategy for adapting the gait to an *OH*-type terrain and its mathematical formulation are described in Section 5, and a strategy for an *OP*-type terrain is defined in Section 6. Section 7 presents a computer simulation of the variation in static stability with terrain type. Finally, Section 8 describes experiments carried out to test the performance of the proposed algorithms using the RIMHO walking robot (Jiménez, González de Santos, and Armada 1993).

2. Crab Straight-Line Walking

2.1. Leg Trajectory in the Support Phase

When a walking robot moves in a given direction, all the legs in the support phase move parallel to that direction. Also, each leg must move with the same speed in relation to the body reference system, to avoid inducing internal forces that cause slipping and changes in body orientation. To simplify the study, some researchers assume that each leg trajectory passes through the central point $\mathbf{C}_i$ of the reachable area, or through the vertical line in the reachable volume that contains that point (Hirose 1984; Lee 1984; Lee and Song 1991).

The reachable volume of a leg is the geometrical locus of all points where a foot can be placed. In the case of a three-dimensional Cartesian-pantograph type leg (the leg of the RIMHO robot) the reachable volume is a rectangular prism. However, as a result of mechanical building requirements, this is an irregular volume (Vargas, Jiménez, and Armada 1991). Also, reachable volumes of collateral legs overlap. To avoid possible leg collisions, a constrained working volume, that is, a rectangular prism, will be considered. The *constrained working volume* is a subset of the total working volume; the *working area* is a section of the constrained rectangular prism (see Figure 1). In this article, we will follow the criterion that the leg remains inside the rectangle that determines the working area. This is correct, independent of the type of terrain, provided that the foot z-coordinate verifies its kinematic limits. The leg trajectory in the support phase can thus be expressed using only x- and y-coordinates.

In addition to the body reference system xyz, the crab reference system $x'y'z'$ is considered. Both systems have coincidental origins with the center of gravity, and the x'-axis is aligned with the direction of motion (see Figure 1). The position of the supporting leg i, for a walking robot utilizing a periodic gait, can be expressed using the concept of local phase, ϕ_{Li}, which provides the normalized time period elapsed from the placement of leg i and the position of the working area center $\mathbf{C}_i$ (Song and Waldron 1987):

$$\begin{bmatrix} x_i'(t) \\ y_i'(t) \end{bmatrix} = [\mathbf{R}_{\mathbf{z},\alpha}]^T \begin{bmatrix} x_{ci} \\ y_{ci} \end{bmatrix} + \begin{bmatrix} \frac{R}{2} - \phi_{Li}(t)\frac{R}{\beta} \\ 0 \end{bmatrix}, \quad (1)$$

where t is the time fraction of a cycle time T after placement of leg i, and the duty factor β is the normalized time period that a leg remains in the support phase. The rotation matrix around the z-axis, $\mathbf{R}_{\mathbf{z},\alpha}$, provides the relationship between the crab reference system and the body reference system, and is given by:

$$\mathbf{R}_{\mathbf{z},\alpha} = \begin{bmatrix} \cos\alpha & -\sin\alpha \\ \sin\alpha & \cos\alpha \end{bmatrix}. \quad (2)$$

The position of $\mathbf{C}_i$ with respect to the body reference system is given by:

$$[x_{ci}, y_{ci}]^T = \begin{cases} [(n-i)\frac{P_x}{2}, \frac{P_y}{2}]^T & \text{if } i \text{ is odd} \\ [(n-i+1)\frac{P_x}{2}, -\frac{P_y}{2}]^T & \text{if } i \text{ is even} \end{cases} \quad (3)$$

where n is half the number of legs and P_x and P_y are the pitch strokes. The stroke R is the maximum distance

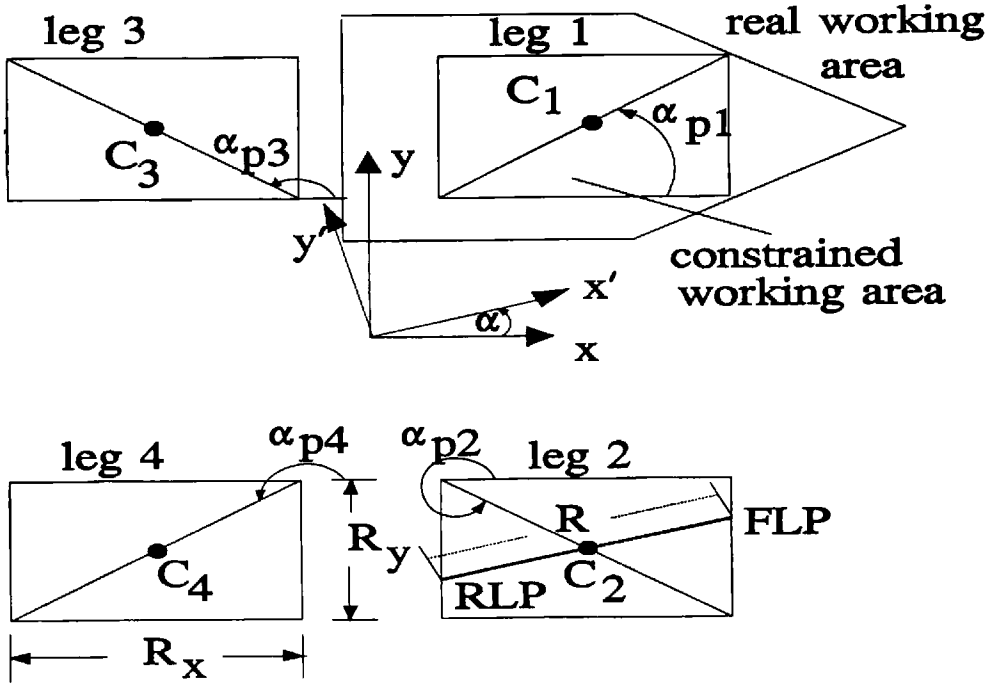

Fig. 1. Leg working areas and reference systems of a quadruped.

provided by the working area for a particular crab angle α, and is defined by (see Figure 1):

$$
\begin{aligned}
R &= \frac{R_x}{\cos\alpha} \quad \text{if } \alpha \le \alpha_{p1} \text{ or } \alpha \ge \alpha_{p2} \\
R &= \frac{R_y}{\sin\alpha} \quad \text{if } \alpha_{p1} < \alpha \le \alpha_{p3} \\
R &= -\frac{R_x}{\cos\alpha} \quad \text{if } \alpha_{p3} < \alpha \le \alpha_{p4} \\
R &= -\frac{R_y}{\sin\alpha} \quad \text{if } \alpha_{p4} < \alpha < \alpha_{p2}
\end{aligned} \tag{4}
$$

where α is the angle between the direction of motion and the longitudinal body axis, and α_{pi} is the angle between the diagonal of the working area of the leg i and the longitudinal body axis. Both angles are measured in a counterclockwise direction.

A supporting leg must move between two positions that will be denoted by *front limit position* (FLP) and *rear limit position* (RLP). The first position corresponds to the intersection point between the stroke trajectory and the working area in the direction of motion. The last position is the intersection point between the stroke trajectory and the working area in the direction opposite to the motion. When the leg touches down, $\phi_{Li}(t) = 0$, the foot is placed at FLP. On the contrary, when the leg lifts up, $\phi_{Li}(t) = \beta$, and the foot is placed at RLP. Both positions can be derived from eq. (1).

2.2. The Transfer Phase

2.2.1. Leg Trajectory in the Transfer Phase

When a leg finishes its support phase (with its foot placed at RLP), it must lift off and transfer forward until it again places its foot at FLP. This is called the transfer phase. Among the multiple leg trajectories in the transfer phase, for simplicity we will consider only one, which consists of three subphases:

1. liftoff subphase,
2. transfer-forward subphase, and
3. placement subphase.

First, the motion of a leg in the transfer phase should be performed in such a way as to avoid collisions with the terrain or any surrounding obstacles. Figure 2*A* shows the trajectory of a foot in relation to a fixed reference system that verifies this condition, which is denoted a *rectangular* trajectory. This trajectory consists of a foot-vertical motion to some predetermined height h (the liftoff subphase); at this point, the foot may be moved to the location above FLP (the transfer-forward subphase); and finally, the foot follows a vertical path to the ground (the placement subphase). However, this foot-rectangular trajectory with respect to a fixed reference system presents some disadvantages in relation to its corresponding trajectory with respect to the body reference system shown in Figure 2*B*.

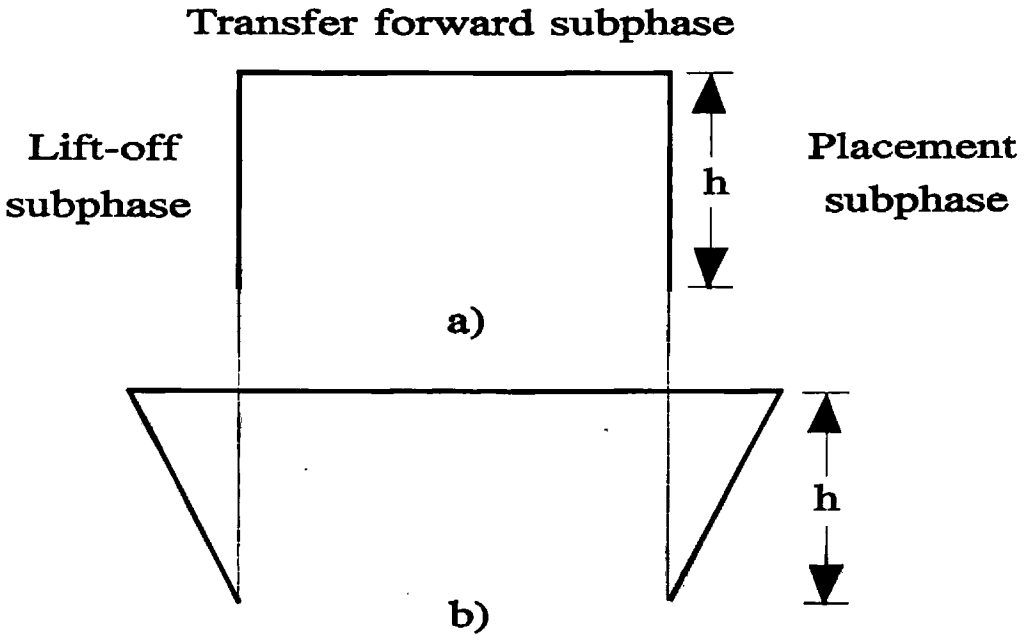

Fig. 2. Rectangular trajectory of a transfer-phase foot with respect to a fixed reference system, A, and its corresponding trajectory with respect to the body reference system, B.

Note that during the liftoff and placement subphases, the leg moves the x-, y-, and z-coordinates with respect to the body reference system. Also, the foot moves in the xy-plane of the body reference system a distance greater than stroke R. The foot must be inside its working volume during its transfer phase, therefore the stroke is constrained. If a vehicle moves using a periodic and regular gait, with a constant speed $v = R/\beta T$, the foot moves in the xy-plane of the body reference system a distance $\lambda = R/\beta$, while the stroke is R (see Figure 3). Therefore, static stability decreases, which is critical for a quadrupedal. In summary, a rectangular transfer-phase trajectory with respect to an external fixed-reference system presents the following disadvantages:

1. greater power consumption than a rectangular trajectory with respect to the body reference system, due to the greater number of actuators moved simultaneously during the liftoff and placement subphases; and
2. limitation of the stroke.

An alternative trajectory without the above disadvantages is a rectangular trajectory in relation to the body reference system (see Figure 4). This trajectory offers the following advantages:

1. greater simplicity in the trajectory generation, and
2. fewer actuators moving at the same time.

However, one drawback is that this trajectory does not avoid collisions with the terrain, since the foot does not move vertically during the first and third subphases with respect to an external reference system. However, this is not so important in the case of a pantographic leg, such as that of the RIMHO walking machine. Figure 5 shows leg motion during the placement subphase and the area swept by the shank when the transferral trajectory is rectangular in relation to an external reference system. This motion is possible if the sweeping area is free of obstacles. In other cases, although the foot cannot collide with the terrain, leg transferral cannot be carried out; therefore, priority is not given to the avoidance of foot collisions when they are caused by the shank. Thus, in accordance with the type of RIMHO robot leg and the advantages presented earlier, a rectangular trajectory with respect to the body reference system was chosen as the transfer trajectory.

2.2.2. Return Time

When a vehicle moves over flat terrain, a leg using the transfer trajectory selected above moves a distance h in both liftoff and placement subphases and a distance R in the transfer-forward subphase. Therefore, the return time of a leg t_r with this rectangular transfer trajectory is given by:

$$t_r = 2\frac{h}{v_z} + \frac{R}{v_{xy}}, \tag{5}$$

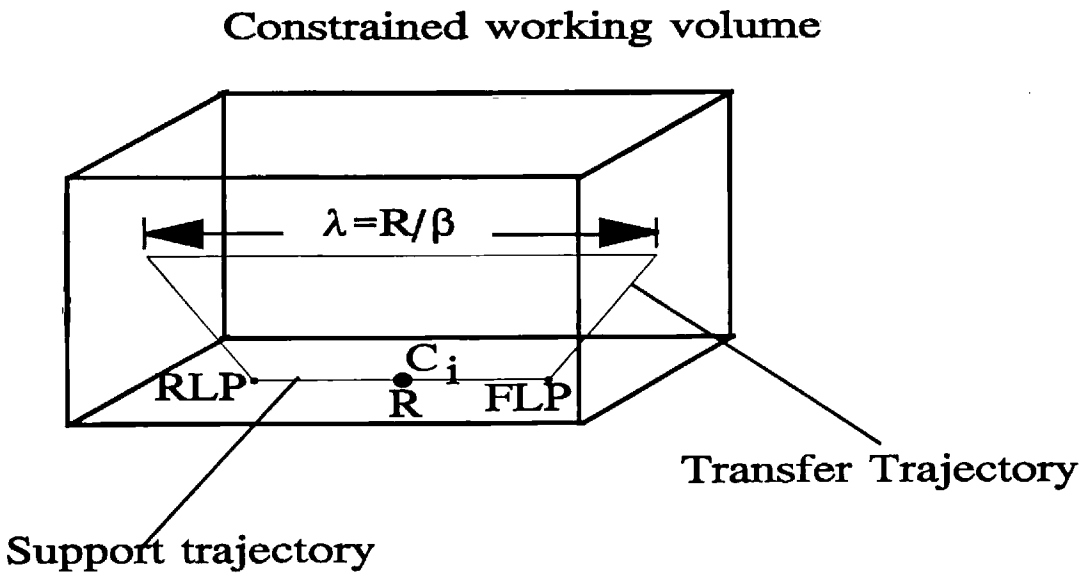

Fig. 3. Working volume and transfer-phase foot trajectory, with respect to the body reference system.

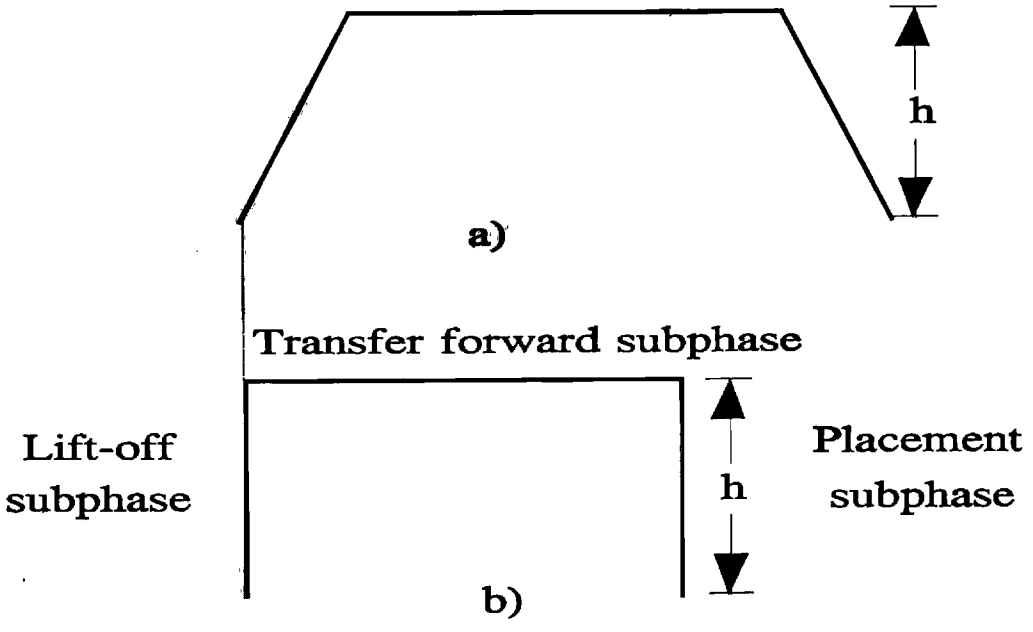

Fig. 4. Trajectory of a transfer-phase foot with respect to a fixed reference system, A, and its corresponding trajectory with respect to the body reference system, B.

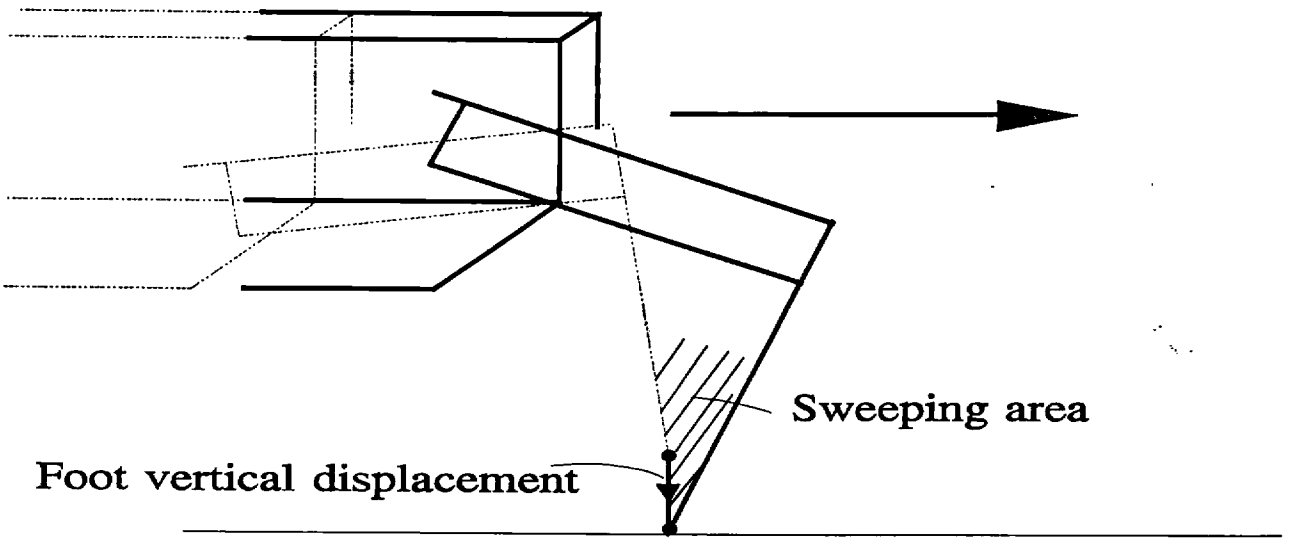

Fig. 5. Motion of a pantographic leg during the transfer phase.

where v_{xy} is the velocity in the xy-plane, and v_z is the velocity along the z-axis. Note that leg acceleration is omitted from this expression and a rectangular velocity profile is considered. In experiments with the RIMHO walking machine (Jiménez 1994), it was shown that in a typical axis motion of 5 s there is an error of 3.1% in the trajectory time, which is considered acceptable for the HCTL-1000 servocontrollers used. For h and R there is a minimum return time due to the maximum velocity of the motors ($v_{z\,\max}$ and $v_{xy\,\max}$), which is given by:

$$t_{r\,\min} = 2\frac{h}{v_{z\,\max}} + \frac{R}{v_{xy\,\max}}. \tag{6}$$

On the other hand, the return time for a periodic and regular gait is related to the time period and the duty factor, as follows:

$$t_r = (1-\beta)T. \tag{7}$$

Therefore, the time period must verify the restriction:

$$T \geq \frac{t_{r\,\min}}{1-\beta}. \tag{8}$$

When using a blind vehicle, the initial time period is calculated using eqs. (6) and (8), as in the case of a flat terrain. If the vehicle moves over an uneven terrain and also the leg stroke varies, a leg in the transfer phase displaces a distance different from both h and R. Considering d_{z1}, d_x, and d_{z3} as the foot displacements in the liftoff, transfer-forward, and placement subphases, respectively, the following expression must be verified:

$$(1-\beta)T = \frac{d_{z1}+d_{z3}}{v_z} + \frac{d_x}{v_{xy}}. \tag{9}$$

If v_{xy} or v_z are greater than $v_{xy\,\max}$ and $v_{z\,\max}$, the time period is not of sufficient duration for the transfer phase. It is, therefore, necessary to increase the time period according to the velocity-control method, which implies a reduction of the body velocity.

3. Irregular Terrain

A gait depends on several factors, such as terrain conditions, stability requirements, smooth body motion, mobility requirements, and speed. Therefore, due to the relationship between gait and terrain, one must define terrain conditions in order to establish adaptive-gait strategy.

Here, we consider an uneven terrain accessible to the walking machine. According to Hirose's classification (Hirose, Iwasaki, and Umetani 1982), this terrain could be modeled as an O-type terrain. However, it is necessary to distinguish whether the ground is above or below a given plane, in order to simplify the adaptative strategy.

In the case of a blind vehicle, only a posteriori-terrain model may be obtained. This is a discrete model, since it is defined by the leg-support positions. It is divided into cells (each the size of a foot) where the foot was or is placed. These cells are on, above, or below the base plane. Thus, a terrain formed by the base plane, holes, and/or protrusions is provided. The base plane is a level plane, and its location with respect to the body reference system is determined by the foot's initial support positions. This plane is used to compute the footholds for the legs in the transfer phase. Therefore, the following classification is proposed for modeling a terrain (see Figure 6):

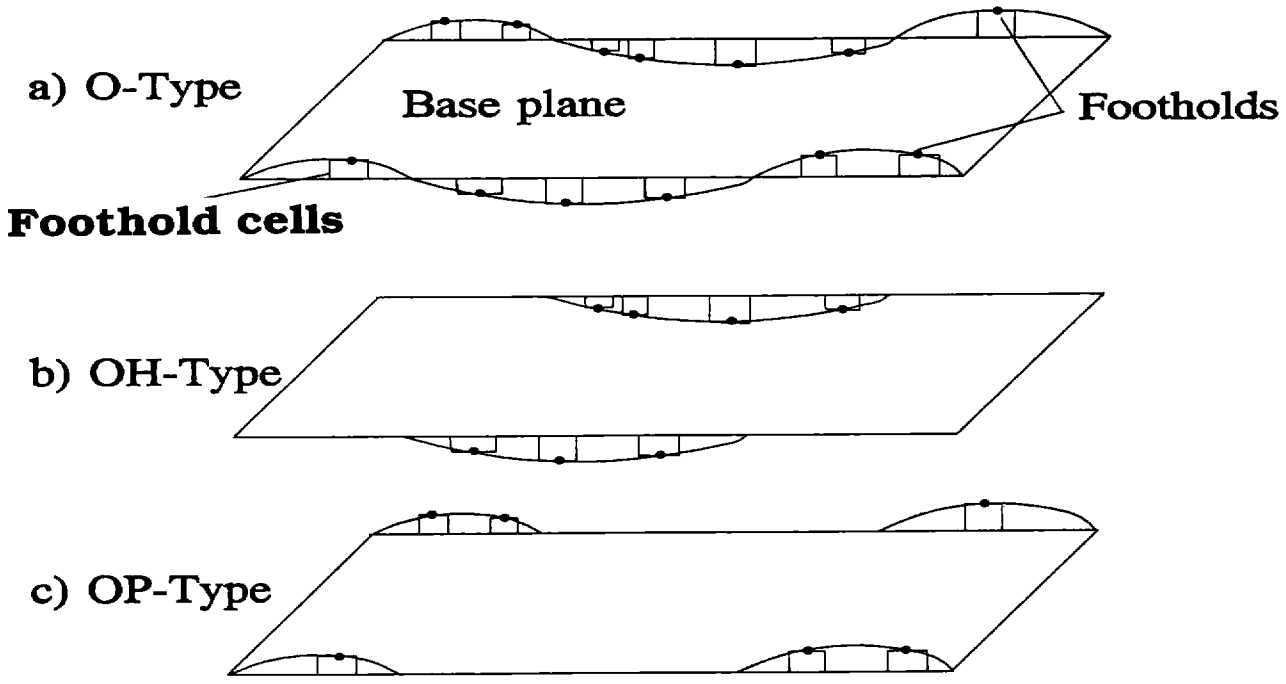

Fig. 6. Classification of terrain.

1. An *O*-type terrain is a ground on which regular walking can be performed without hindrance. It is a discrete ground with respect to the base plane.
2. An *OH*-type terrain is the base plane containing holes.
3. An *OP*-type terrain is the base plane containing protrusions.

Therefore, the *O*-type terrain results from the union of the other two terrain types, *OH*-type and *OP*-type.

4. Methods of Controlling Gait Parameters

This section describes the two methods of controlling gait parameters that are used to adapt a periodic gait to an *O*-type terrain. One method enables the stroke to be modified while maintaining a constant speed. The other permits the body velocity to be decreased, thus increasing the time period.

4.1. The Stroke-Control Method

This method allows the stroke to be modified while maintaining a constant speed. It is based on a method proposed by Kumar and Waldron (1989), for adapting the gait to previously selected footholds. This method increases stroke, R_0, and time period, T_0, while duty factor, β, and body speed, v_0, remain constant. Leg kinematics must not, then, restrict stroke; i.e., the initial stroke, R_0, must be lower than the maximum leg stroke, $R_{\max}$.

Moreover, to maintain constant speed, the new stroke, R_1, and new time period, T_1, must verify the following expression:

$$v_0 = \frac{R_0}{\beta T_0} = \frac{R_1}{\beta T_1}, \tag{10}$$

where T_1 verifies the following restriction:

$$T_1 \geq \frac{T_{r\min}}{1-\beta}. \tag{11}$$

Therefore, the new stroke, R_1, must verify the following inequality:

$$\frac{R_0 t_{r\min}}{T_0(1-\beta)} \leq R_1 \leq R_{\max}. \tag{12}$$

The *O*-type terrain-adaptive strategy, proposed here, does not require the x- and y-coordinates of the foothold FLP to be modified. However, to adapt the foot's z-coordinate to the ground, either the support time or the transfer phase must be increased. When a leg is placed on the top of a protrusion (*OP*-type terrain), its support time is increased; yet, when a leg finishes its transfer phase before reaching the ground (*OH*-type terrain), its return time is increased. To reach this objective, the stroke is increased according to eq. (12) while keeping the time period constant. This restriction is imposed to recover initial locomotion, which is defined by R_0, T_0, and β gait parameters.

In the case of an *OH*-type terrain, the hole height is unknown. At first, an arbitrary value of R_1 that verifies condition (12) is chosen, but this does not ensure that a

leg can contact the ground. Also, the new stroke must be such that the static stability margin is a positive value.

4.2. The Velocity-Control Method

The time period determines the return time for a periodic gait. Also, the return time is limited by the dynamic capacity of the joint servomotors, and is a function of the distance that the leg covers during its transfer phase. Therefore, when the time period is not sufficient for the transfer phase to take place, it is increased in such a way that the restriction of the minimum return time is verified.

If, for example, for a given time period T_0, leg velocity during the transfer-forward subphase is:

$$v_{xy} \geq v_{xy\,\max}, \tag{13}$$

it is necessary to calculate the new time period T_1, in such a way that verifies that the return time is greater than the minimum value. The time period T_1 must be greater than T_0, by a certain factor, according to the expression:

$$T_1 = \mu T_0, \tag{14}$$

where the factor μ is given by [see eq. (13)]:

$$\mu = \frac{v_{xy}}{v_{xy\,\max}}. \tag{15}$$

At the same time, the body velocity must decrease by the same factor μ:

$$v_1 = \frac{v_0}{\mu}. \tag{16}$$

In the following sections, we present two possible strategies for adapting a periodic gait to an O-type terrain using the above-mentioned methods for controlling gait parameters. The OH-type and OP-type terrains are considered separately.

5. An OH-Type Terrain-Adaptive Gait

5.1. Strategy

When a leg j reaches its final position without touching the ground, this leg must be placed before the corresponding leg i lifts off. It is thus necessary to increase its return time (extra-return time). To do so, the stroke R_0 is increased to R_1 for the legs in the support phase, according to the aforementioned stroke-control method, keeping the leg-stroke center constant. This increase of the stroke is called *hollow control over leg j*. While the legs in the support phase move to their new final positions defined by R_1, NRLP, leg j descends a distance h_e along a vertical trajectory with respect to the body reference system. This algorithm is repeated until leg j touches the ground if static stability is maintained and conditions for applying the stroke-control method are verified. Otherwise, vehicle motion must be stopped until leg j contacts the ground (see Figure 7).

In this strategy, it is desirable to recover the initial stroke R_0, thus permitting the adaptive-gait control to be performed more times. On the other hand, when leg j contacts the ground, the other legs in the support phase move to their new final positions NRLP. On the other side, the leg j must move a distance R_0 from its current position FLP-R_0 to RLP-R_0.[1] When any of the legs has started the transfer phase, it must move to the final position FLP-R_0 in the return time $t_r = (1 - \beta)T_0$. When it is in the support phase, it will move to the final position RLP-R_0. Therefore, when leg j finishes its support phase, the stroke will again be R_0. If, before recovering the initial stroke, it is necessary to carry out another hollow control maneuvre over another leg, the stroke must increase from R_1 to R_2. The stroke will recover its initial value when hollow control has been performed over the last leg and the support phase is finished.

In the following section, the mathematical formulation related to this strategy is presented. First, we discuss the type of trajectory for leg j in the air after finishing its return time. We then establish the formula that describes the time that the leg j remains in the air and the restrictions that must be verified. Finally, we present a mathematical formula describing the motions of the other legs.

5.2. Extra-Transfer Phase

The time that a leg remains in the air after finishing its transfer phase is denoted as the *extra-transfer phase*. The duration of this phase is called the *extra-return time*, $t_{re,j}$. Now the problem of selecting the most adequate trajectory in the extra-transfer phase arises. Initially, two basic trajectories with respect to the body reference system can be considered: the *step trajectory* and the *straight trajectory*. The step trajectory consists of two subphases, transfer forward and placement, while the straight trajectory consists of a unique placement phase.

5.2.1. Selection of the Leg Trajectory in the Extra-Transfer Phase

If the leg over which the hollow control is carried out is a rear leg, the step trajectory presents some advantages over the straight trajectory, based on the static stability. To explain this point, we must consider that the longitudinal (or transversal) stability margin in a locomotion cycle is the minimum of the front longitudinal (transversal) stability margin just before a leg is placed, or the minimum of the

1. FLP-R_0 is the FLP when the stroke is R_0, while FLP-R_1 is the FLP when the stroke is R_1.

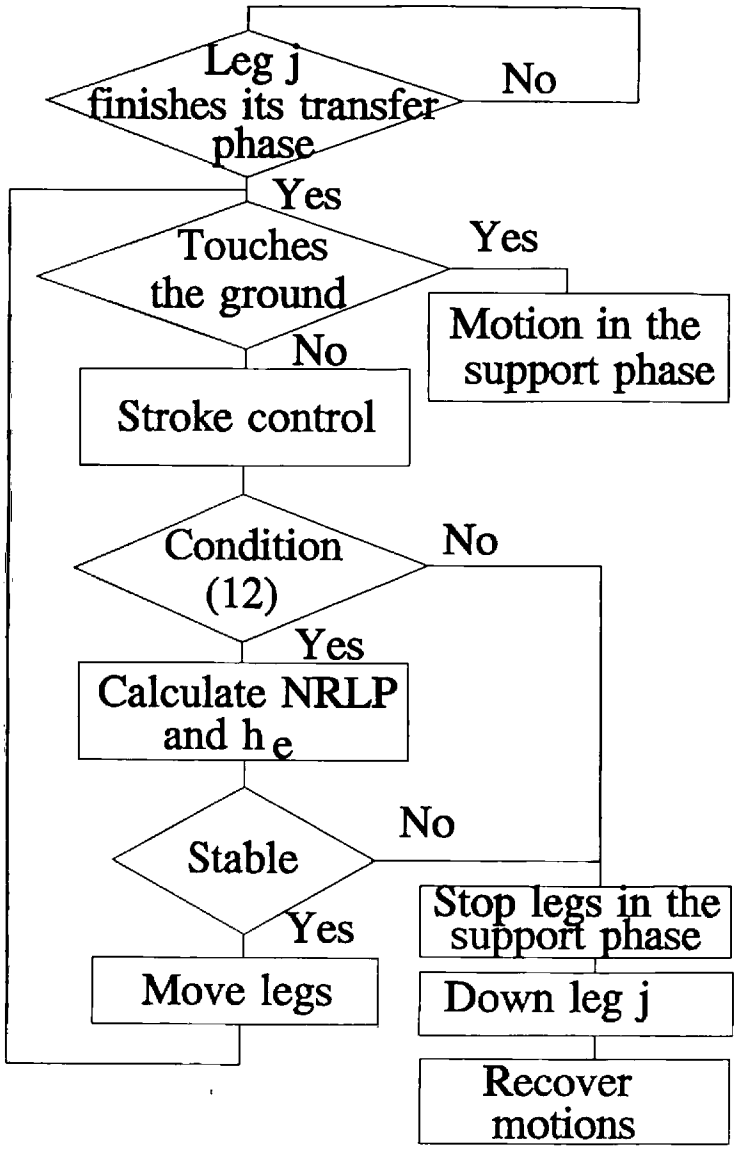

Fig. 7. Flow chart of the hollow control over a leg j.

rear longitudinal (transversal) stability margin just after a leg is lifted (Zhang and Song 1990). The hollow control over a rear leg increases the rear longitudinal (transversal) stability margin just before the leg makes contact with the ground; it also decreases the front longitudinal (transversal) stability margin just before the front leg of the same side is placed. This measure of the static stability depends on the type of trajectory of the rear leg during the extra-transfer phase, so the minimum longitudinal (or transversal) stability margin can change. When the leg that remains in the air after finishing its transfer phase is a front leg, the front longitudinal (transversal) stability margin decreases while the hollow control is performed over that leg. This implies a decrease in the longitudinal (transversal) static stability in a locomotion cycle. In such a case, the type of leg trajectory in the extra-transfer phase does not affect the gait longitudinal (transversal) stability margin. The following shows how the type of extra-transfer trajectory affects the longitudinal stability margin when a unique hollow control over a rear leg is performed.

A quadruped vehicle moving with a wave gait whose parameters are $\beta = 3/4, \alpha = 0°$, and stroke R_0 is considered. Figure 8 shows the corresponding gait diagram and stationary gait pattern for flat terrain. Figure 9 compares support patterns when hollow control is carried out over leg 4, in the time just before leg 2 finishes its transfer phase, for the two cases of step and straight extra-transfer trajectories. If leg 4 remains in the air when the transfer phase is completed, the stroke is increased to R_1 to

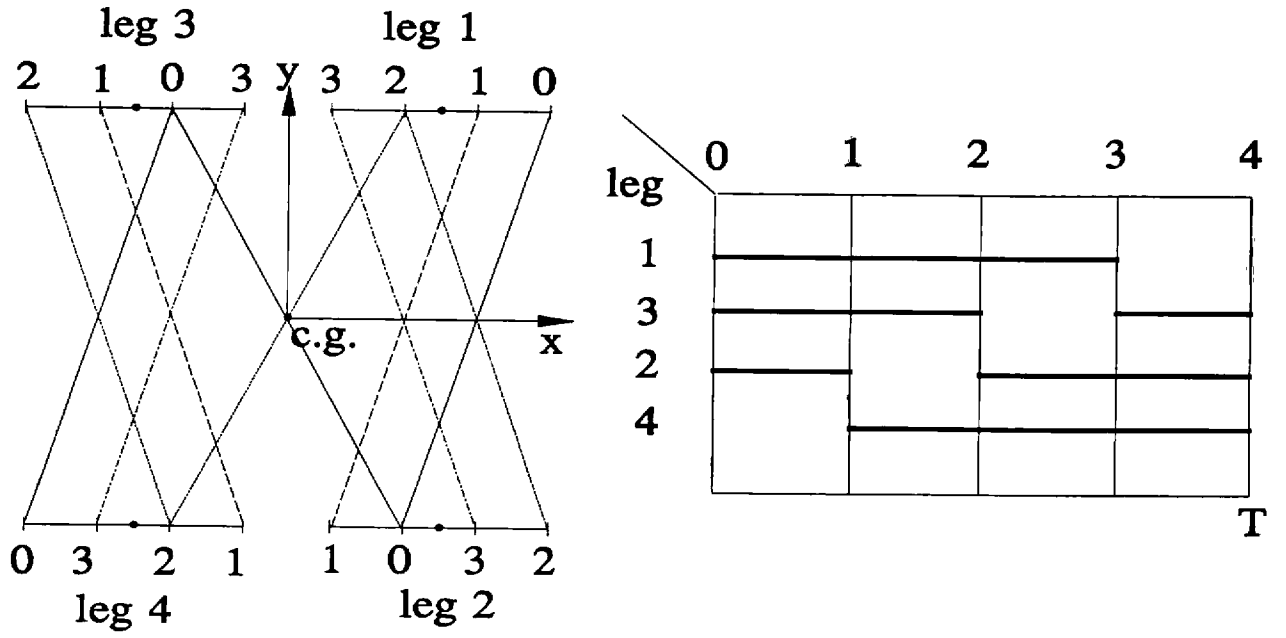

Fig. 8. Stationary gait pattern and gait diagram for the wave gait with $\beta = 3/4, \alpha = 0°$, and flat terrain.

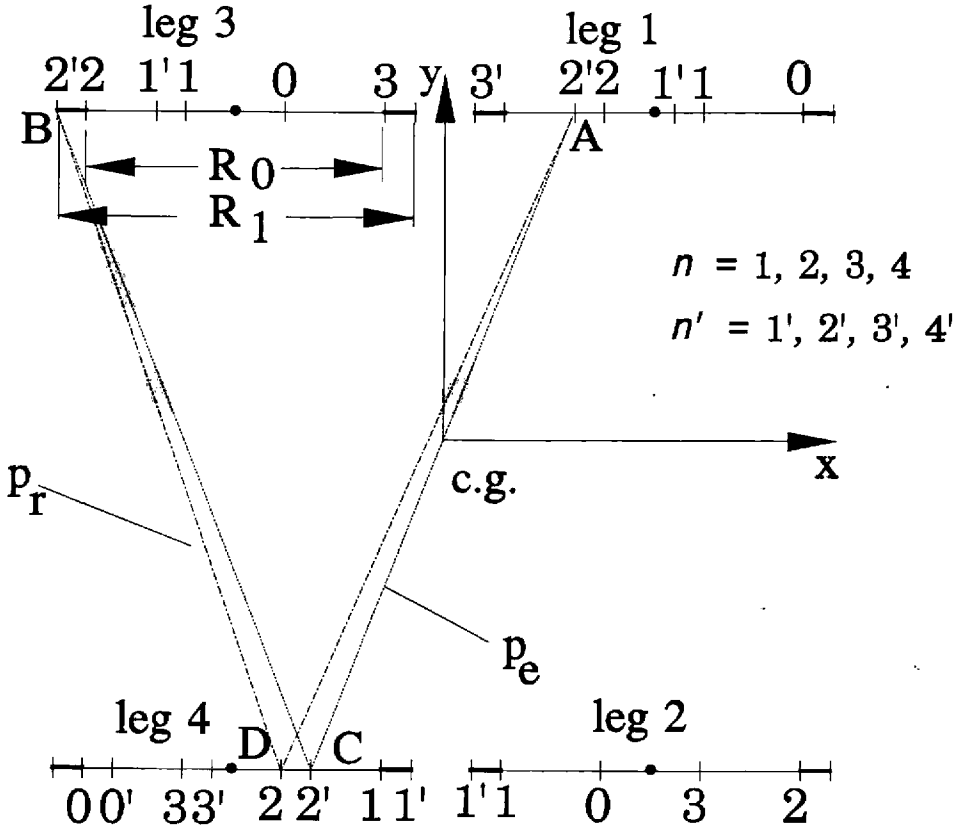

Fig. 9. Comparison of the stationary gait pattern for the two cases of the extra-transfer trajectory: step trajectory and straight trajectory.

reach the ground. In Figure 9, n represents the foot position when the stroke is R_0, and n' represents the foot positions when the stroke is increased to R_1.

In the case of the step trajectory, leg 4 must move from position PLD-R_0 (position 1) to position PLD-R_1 (position 1′), in which leg 4 is assumed to make contact with the ground; therefore, just before leg 2 touches the ground (position 2), leg 4 is at the position denoted by 2′ and the support pattern is denoted by p_e (its vertices are A, B, and C). However, in the case of a straight trajectory, leg 4 contacts the ground in the position 1; therefore, just before leg 2 contacts the ground, leg 2 is in position 2 and the support pattern is p_r (with vertices A, B, and D). As can be seen in the figure, the stability longitudinal margin corresponding to the support pattern p_e remains equal to the case of flat terrain (see Figure 8) in the time just before leg 2 touches the ground. However, the stability longitudinal margin corresponding to the support pattern p_r is very different to that shown in Figure 8. In this case the center of gravity is outside the support pattern, which is an unstable situation. Therefore, the step trajectory ensures static stability while the straight trajectory does not.

The straight trajectory presents two disadvantages derived from the transfer-forward subphase, however. Although the foot is in the air, it is not at a minimum height to ensure no collisions during the transfer-forward subphase. Still, it is convenient to consider that the transfer-forward displacement of a leg over which hollow control is performed depends on whether hollow control over other legs has been carried out in the same locomotion cycle. In this case, the forward displacement increases, and as the return time is immovable, the displacement in the z-axis decreases. Therefore, more hollow control over the same leg would be necessary to reach the ground. These drawbacks lead us to consider the straight trajectory as the most adequate in the extra-transfer phase. However, to avoid static stability problems, the duty factor must be greater than $\beta = 3/4$.

5.2.2. *Extra-Return Time*

The straight-type extra-transfer phase exists in the motion of the z-axis from the current position until the foot touches the ground. In this phase, the foot will translate an unknown distance h_e. The extra-return time of the leg j is then given by:

$$t_{re,j} = \frac{h_e}{v_z}. \tag{17}$$

Moreover, this time is determined by the distance moved by the legs in the support phase, while the leg j descends to the ground and the body velocity is v_0. Considering that the stroke center does not vary, the distance moved by the legs in the support phase is half of the difference between the new stroke R_n and the immediately previous stroke R_{n-1}. When only one stroke control is performed, the new stroke is R_1 and the previous stroke is the initial stroke, R_0. In general, the extra-return time is given by:

$$t_{re,j} = \frac{\frac{R_n - R_{n-1}}{2}}{v_0}. \tag{18}$$

Combining eqs. (17) and (18), the following expression is obtained:

$$h_e = \frac{(R_n - R_{n-1})v_z}{2v_0}, \tag{19}$$

which provides the height that a leg can descend as a function of R_n, R_{n-1}, v_0 and v_z. Considering the maximum velocity at the z-axis to be $v_{z\,\max}$ the extra maximum height is given by:

$$h_e \leq \frac{(R_n - R_{n-1})v_{z\,\max}}{2v_0}. \tag{20}$$

This height is limited by the kinematic limits:

$$h_{e,\max} = H_0 - H_{\min} > 0, \tag{21}$$

where $H_{\min}$ is the minimum z-coordinate that can reach the foot with respect to the body reference system, and H_0 is the height of the base plane with respect to the same reference system.

5.3. *Motion Coordination*

When the stroke is modified so that the leg remaining in the air reaches the ground, the final position of each leg in the support phase is modified. In coordinates of the crab system, these positions are given by:

$$\begin{bmatrix} x_i' \\ y_i' \end{bmatrix}_{\text{NRLP}} = \begin{bmatrix} x_i' \\ y_i' \end{bmatrix}_{\text{ORLP}} - \begin{bmatrix} \frac{R_n - R_{n-1}}{2} \\ 0 \end{bmatrix}; \quad i = 1,\ldots,4; \quad i \neq j, \tag{22}$$

where ORLP is the position at the end of the support phase before changing the stroke, and $(R_n - R_{n-1})/2$ is the distance displaced by the legs in the support phase during the extra-transfer phase of the leg j. If R_n is the stroke as the leg j reaches the ground, this leg will move to the position RLP-R_0. Each leg in the support phase that reaches its final position will move to the position FLP-R_0 as given by:

$$\begin{bmatrix} x_i' \\ y_i' \end{bmatrix}_{\text{FLP}-R_0} = [R_{z,\alpha}]^T \begin{bmatrix} x_{ci} \\ y_{ci} \end{bmatrix} + \begin{bmatrix} \frac{R_0}{2} \\ 0 \end{bmatrix}. \tag{23}$$

The final position of each leg in the support phase will be modified when a hollow control is performed over the leg in the transfer phase.

Each leg in the transfer phase covers a distance $d = dist((x_i', y_i')_{\text{NRLP}}, (x_i', y_i')_{\text{FLP}-R_0})$ in the xy-plane. The return time must be such as to ensure a statically stable gait. While one leg is in the transfer phase, the rest of the legs must be in the support phase. Figure 9 shows that while leg 2 is in the transfer phase between the positions labeled 1′ and 2, leg 3 moves in the support phase between the positions 1′ and 2′. This distance is determined by the initial stroke R_0 and the duty factor β, according to the expression $R_0(1-\beta)/\beta$ (in this particular case, $\beta = 3/4$ and the distance between 1′ and 2′ is $R_0/3$). Besides, this is equal to the distance of a leg in the support phase moving with a speed $v_0 = R_0/\beta T_0$ in a time $(1-\beta)T_0$. For the velocity to remain constant to v_0, the return time must be equal to $(1-\beta)T_0$. Consequently, the time period T_0 must be maintained while the stroke control is performed. Once the transfer phase is finished, the legs will move in the support phase until each reaches the final position RLP-R_0.

5.3.1. Example

A quadruped that moves with a wave gait and parameters $\beta = 5/6, \alpha = 0°, R_0$, and T_0 is considered. Figure 10 shows the gait diagram and the stationary gait pattern for the wave gait assuming flat terrain and constant body velocity v_0. Quadrilaterals at times denoted by 0, 1, 2, 3, 4, and 5 are shown; also, at times 1, 3, and 4 (in which static stability is more critical), the support triangles from just after a leg lifts off or just before a leg places are drawn.

Now, an irregular *OH*-type terrain is considered, and it is presumed that leg 4 does not touch the ground after finishing its transfer phase. The stroke is then increased to R_1 until leg 4 reaches the ground. Figure 11 shows the gait diagram of the wave gait for flat terrain (solid lines) and its modification to perform the hollow control for leg 4 (dotted lines). It shows the time between 2 and 2′ in which leg 4 touches the ground. Figure 12 shows the corresponding stationary gait pattern. The static stability in the locomotion cycle after time 2′ is maintained, as can be observed graphically.

6. An *OP*-Type Terrain-Adaptive Gait

When a leg j in the transfer phase contacts the ground before its final position is reached, its support time must be increased in order to avoid instability. To do so, the stroke of the leg j is increased to R_1, which is denoted as *protrusion control over leg j*. Once this leg finishes its support phase, the stroke will recover its initial value R_0. The time period, T_0, and stroke of the rest of the legs, R_0, remain constant.

The new leg stroke R_1 is calculated considering the symmetry of the stroke with respect to center $\mathbf{C}_j$, according to this expression:

$$R_1 = R_0 + 2t_m v_0 \tag{24}$$

where t_m is the time of early contact with the ground. It is given by one of the following equations, depending on whether contact with the soil occurs during the placement subphase or the transfer-forward subphase:

$$t_m = \frac{z_t - z_r}{v_z}, \text{ or} \tag{25}$$

$$t_m = \frac{z_t - z_r}{v_z} + \frac{\sqrt{(x_t - x_r)^2 + (y_t - y_r)^2}}{v_{xy}}, \tag{26}$$

where x_t, y_t, and z_t are the theoretical positions of the x-, y-, and z-axes at the end of the transfer phase; and x_r. y_r, and z_r are the x-, y-, and z-axis positions when the foot touches the ground.

The new final position, with respect to the crab reference system, for a leg over which protrusion control is performed, is given by:

$$\begin{bmatrix} x_j' \\ y_j' \end{bmatrix}_{\text{NRLP}} = \begin{bmatrix} x_j' \\ y_j' \end{bmatrix}_{\text{RLP}-R_0} - \begin{bmatrix} t_m v_0 \\ 0 \end{bmatrix} \tag{27}$$

Note that if after performing protrusion control over a leg k, hollow control over a leg j is carried out, the new position NRLP of the foot k is calculated using eqs. (27) and (22). Figure 13 shows the flow chart of the protrusion-control algorithm over a leg j.

6.1. Example

A quadruped vehicle moving with wave-gait parameters $\beta = 5/6, \alpha = 0°$, stroke R_0, and time period T_0 over an *OP*-type terrain is considered. Figure 14 shows the gait diagram for the case in which leg 4 places on a protrusion. The corresponding stationary gait pattern is shown in Figure 15.

7. Simulation Study of Static Stability

Automatic adaptation of a quadruped vehicle motion to an irregular terrain using the terrain-adaptive gait algorithms presented here will be shown with several examples. The simulation results show the longitudinal stability margin as a function of the time, over three locomotion cycles. This measure of stability is determined (a) at the time just before (the four legs in the support phase) and after (three legs in the support phase) the support phase of a leg is finished; (b) when a leg finishes its transfer phase and remains in the air; (c) each time a leg finishes its extra-transfer phase; and (d) just before (three legs in

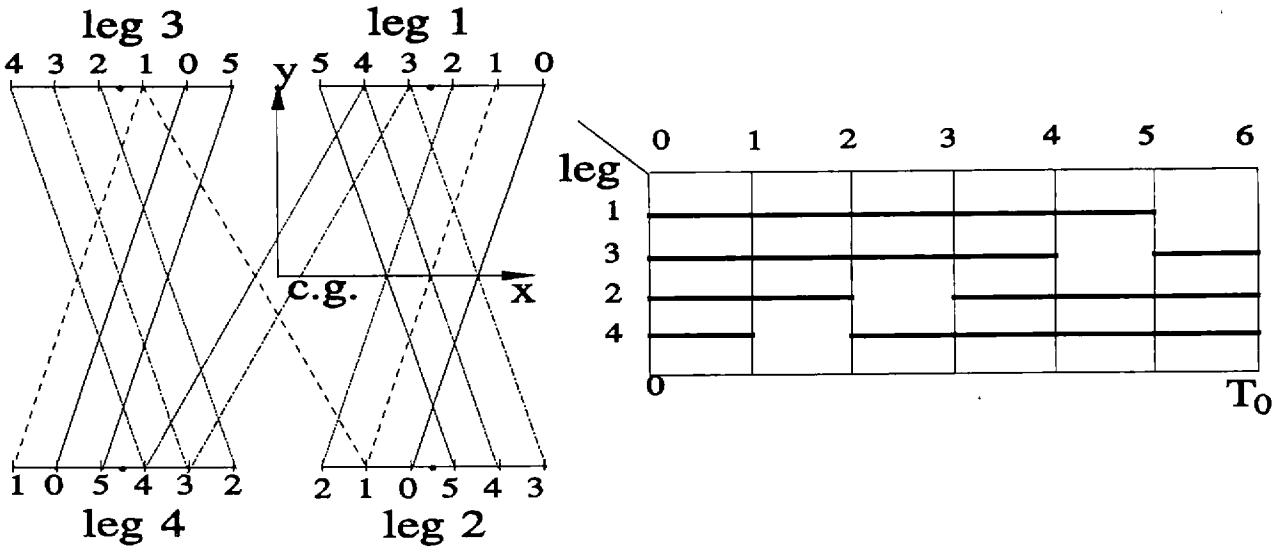

Fig. 10. Stationary gait pattern and gait diagram for the wave gait with $\beta = 5/6, \alpha = 0°$, and flat terrain.

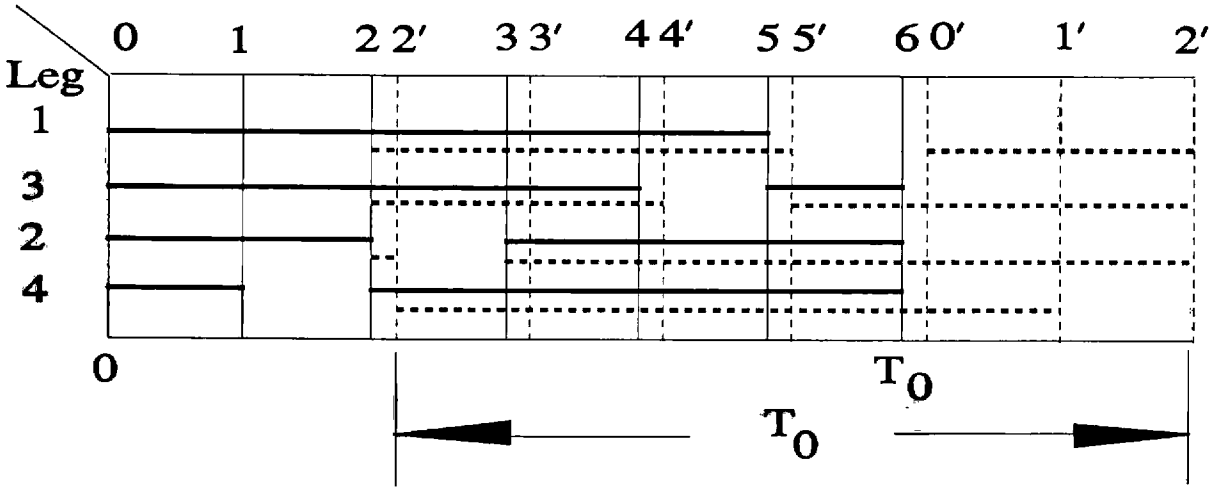

Fig. 11. Gait diagram for the wave gait with $\beta = 5/6, \alpha = 0°$, and OH-type terrain.

the support phase) and after (four legs in the support phase) touching the ground. Since straight-line motion is considered, the longitudinal stability margin varies linearly and the values calculated at the times specified above can be joined by straight lines.

In this simulation study, the constrained working area with dimensions $R_x = 500\,\text{mm}$ and $R_y = 200\,\text{mm}$ and pitch strokes $P_x = 700\,\text{mm}$ and $P_y = 100\,\text{mm}$ are considered. The maximum constrained working volume that can be obtained from the real working volume has the dimensions $R_x = 600\,\text{mm}$, $R_y = 300\,\text{mm}$, and $R_z = 314\,\text{mm}$. The base plane considered here is placed at a distance of $H_0 = 400\,\text{mm}$ with respect to the body reference system and the minimum z-coordinate reachable by a leg is given as $H_{\text{min}} = -491\,\text{mm}$.

Figure 16 shows the longitudinal stability margin of the wave gait with duty factor $\beta = 0.77$, crab angle $\alpha = 0°$, velocity $v_0 = 9\,\text{mm/s}$, stroke $R_0 = 500\,\text{mm}$, and time period $T_0 = 72.15\,\text{s}$, over flat terrain. This figure shows the time at which the longitudinal stability margin is calculated, in the first locomotion cycle, by the symbols *fsn* and *ftn*. The *fsn* symbol corresponds to the time just after the support phase of the leg n is finished, while *ftn* corresponds to the time just before the transfer phase is finished. As can be observed, each time has associated values of LSM: the greater value corresponds to the case in which the four legs are in the support phase, while the smaller value corresponds to the case in which only three legs are in the support phase. The minimum longitudinal stability margin occurs at the times *fs4*, *ft2*, *fs3*, and *ft1*,

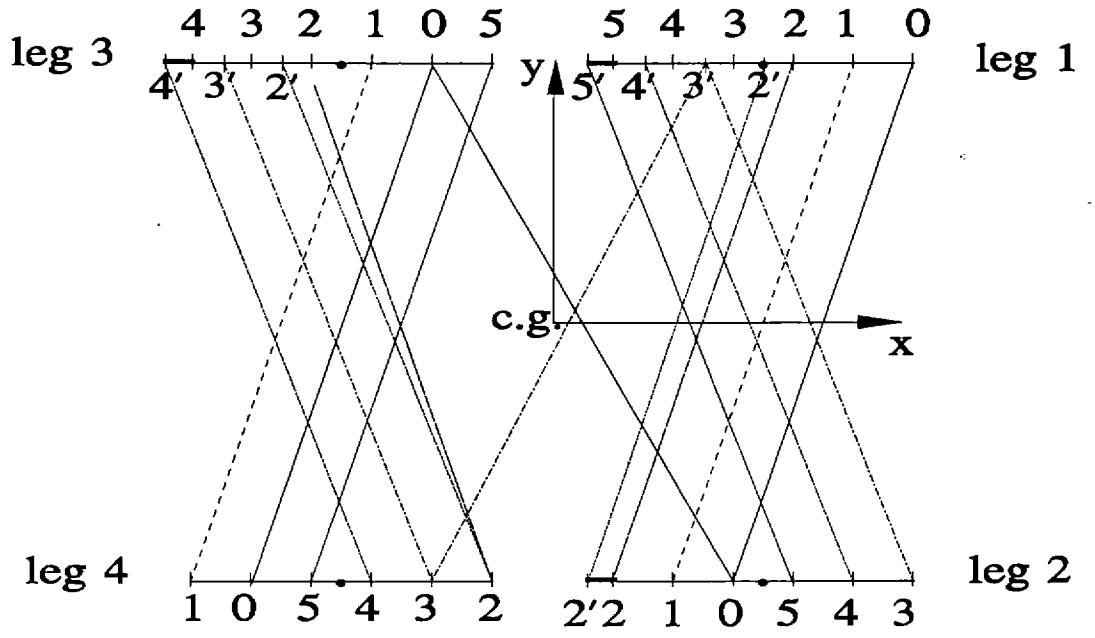

Fig. 12. Stationary gait pattern for the wave gait with $\beta = 5/6, \alpha = 0°$, and OH-type terrain.

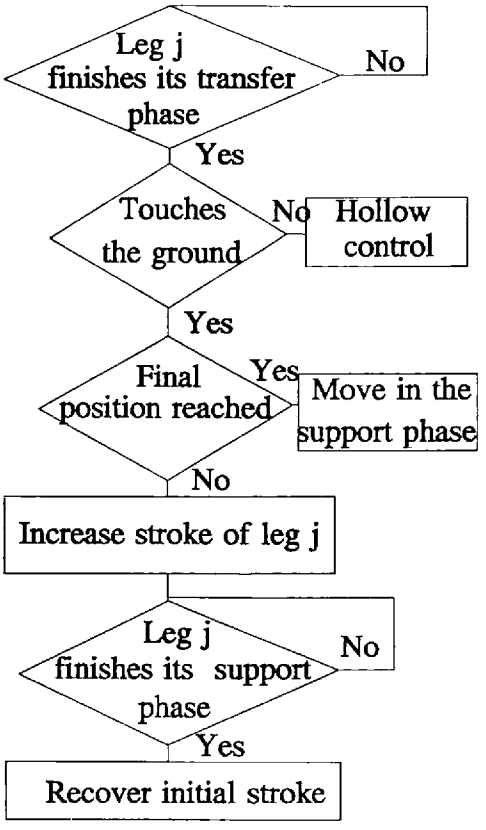

Fig. 13. Protrusion-control algorithm over a leg j.

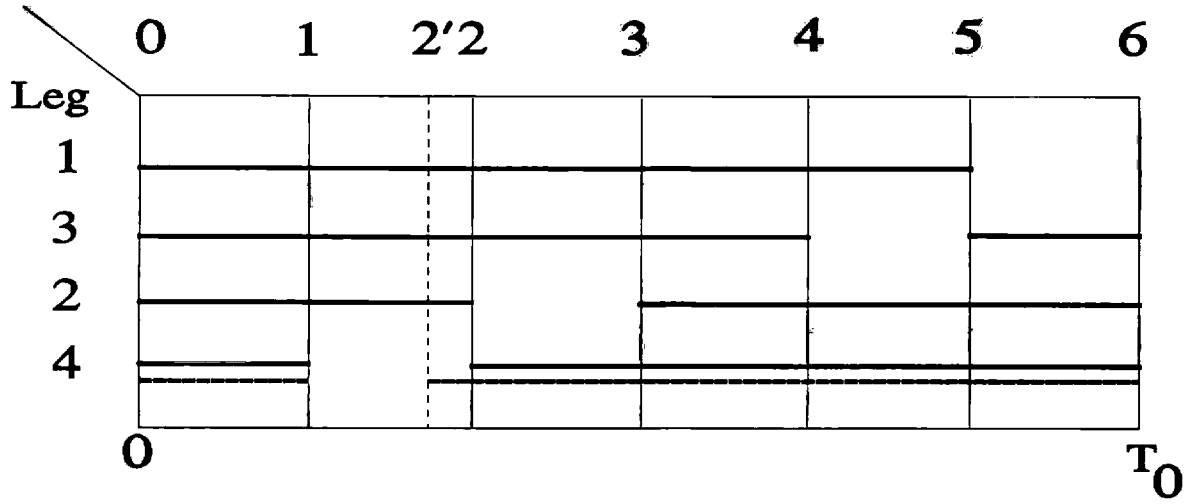

Fig. 14. Gait diagram for the wave gait with $\beta = 5/6$ and $\alpha = 0°$ over OP-type terrain.

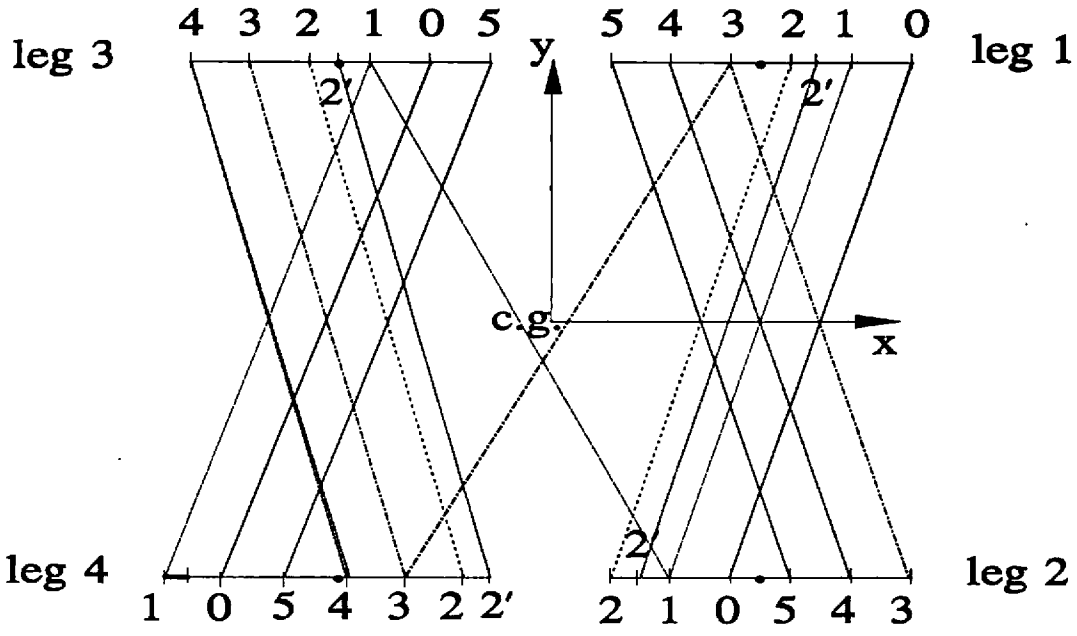

Fig. 15. Stationary gait pattern for the wave gait with $\beta = 5/6$ and $\alpha = 0°$ over OP-type terrain.

i.e., just after a rear leg finishes its support phase and just before a front leg touches the ground, and its value is equal to 12.98 mm. In this case, the results obtained in the other locomotion cycles are the same.

Figure 17 shows the LSM in the case of an *OH*-type terrain, where it is necessary to perform hollow control over the two front legs, 1 and 2. The depression height for each of the legs is 30 and 20 mm, respectively. In this case, leg 2 does not contact the ground after finishing its transfer phase (denoted by *nc2*). Then, the initial stroke must increase by 12 mm ($R_1 = 512$ mm) so that leg 2 reaches the ground before leg 3 finishes its support phase. This produces a decrease of the minimum LSM when leg 2 touches the ground (*c*2). Also, an increase of the LSM at the time *fs3* with respect to its value in the case of flat terrain is produced. However, this value does not improve the gait longitudinal stability margin, as commented in Section 5.2.1. Before recovering the initial stroke, it is necessary to perform another hollow control over leg 1. This means that at the time in which leg 1 touches the ground, *c*1, the stroke is $R_2 = 528$ mm. Therefore, between the times *nc*1 and *c*1, the LSM decreases with respect to the value at the time *c*2. The difference between the results obtained in the first and in the rest of the locomotion cycles lies in the LSM at the time *fs4*. This difference is due to the fact that the stroke in the

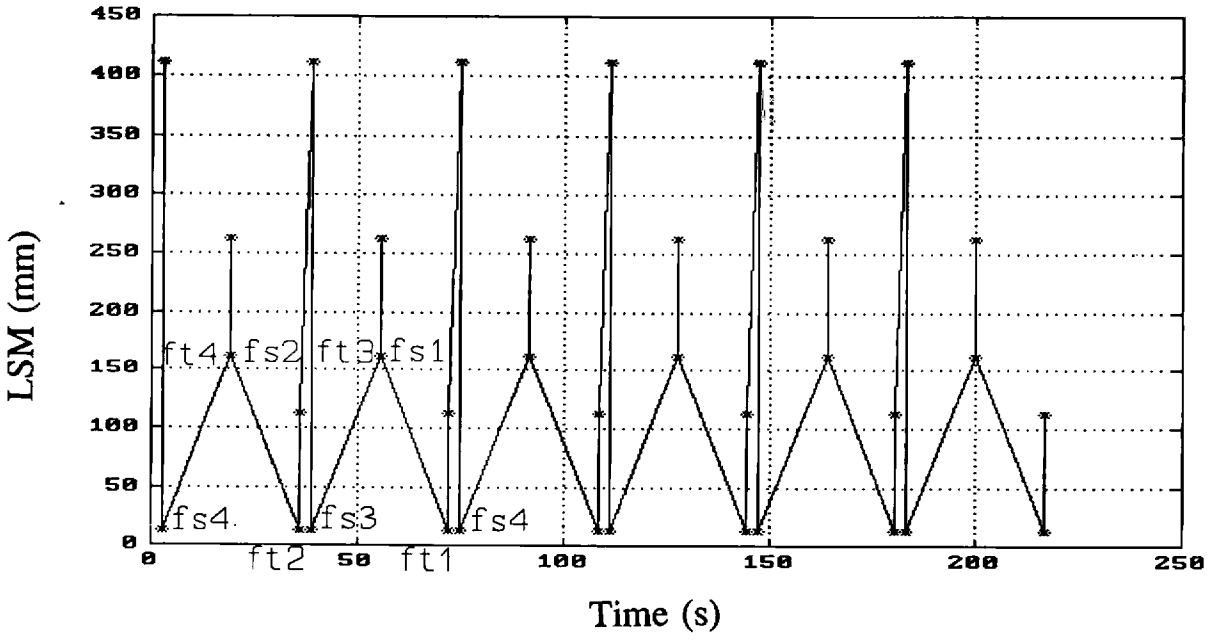

Fig. 16. Longitudinal stability margin for a wave gait with $\beta = 0.77$ and $\alpha = 0°$ over flat terrain.

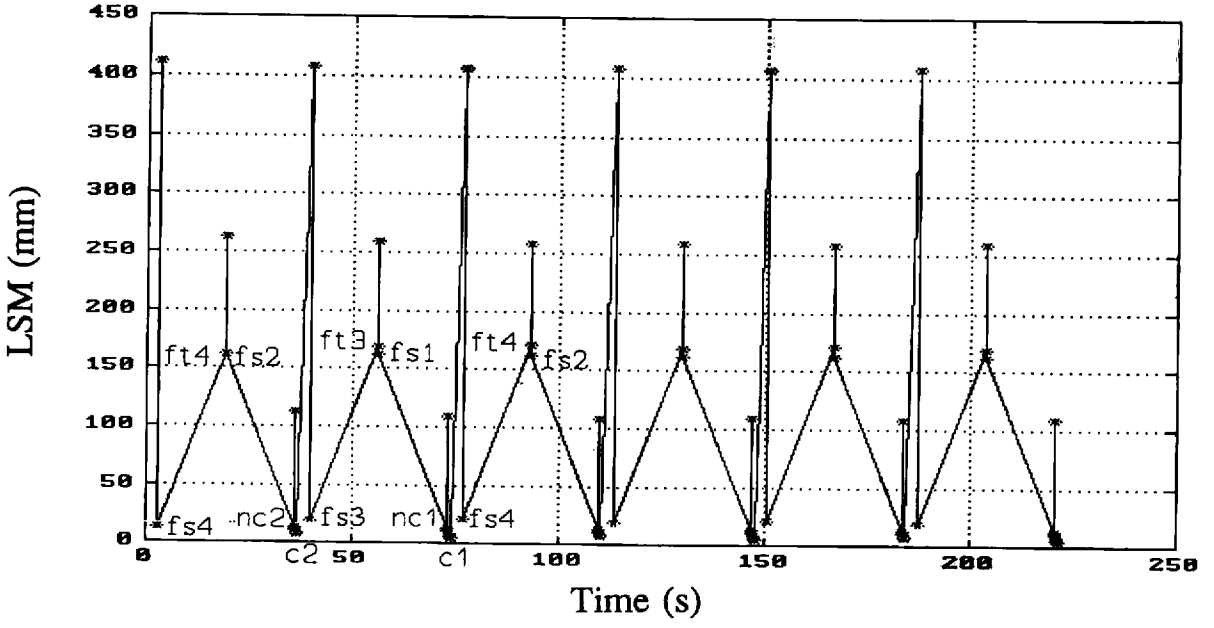

Fig. 17. Longitudinal stability margin for a wave gait with $\beta = 0.77$ and $\alpha = 0°$, and hollow control over legs 1 and 2.

first locomotion cycle, when leg 4 finishes its support phase, is R_0; the stroke in the second locomotion cycle at this event is 28 mm greater.

Figure 18 shows the simulation results in the case of an O-type terrain. In this terrain, protrusion control is performed over legs 2 and 3, whereas hollow control is realized over leg 4. The protrusion heights are 20 mm, while the depression height is 30 mm. For leg 4 to reach the ground, we must increase the stroke by increments of 4 mm to $R_4 = 516$ mm. According to eq. (19), the height of the depression with the parameters $R_0 = 500$ mm, $v_0 = 9$ mm/s and $v_z = 35$ mm/s is $h_e = 31.11$ mm. Since the depression height is 30 mm, the leg stopped before reaching the calculated height. Therefore, it is necessary to perform a protrusion control over leg 4. It is noteworthy that in the previous example, protrusion control was performed after hollow control. When leg 2 finishes its transfer phase, its stroke increases to $R_1 = 510.28$ mm according to eqs. (24), (25), and (26). The same procedure is followed when leg 3 finishes its transfer phase. Due to the aforementioned hollow and protrusion controls, the gait longitudinal stability margin decreases with respect to the corresponding value in the case of flat terrain.

8. Experimental Results

This section shows some experimental results obtained with the RIMHO walking machine (see Figure 19), with the aim of verifying the proposed adaptive-gait algorithms. In the previous section, the LSM behavior in the adaptive-gait algorithms was presented. Its experimental behavior would be the same in the case of an ideal vehicle. However, mechanisms introduce many variations to the geometrical model and the experimental results, apart from the theoretical results masking some results related to periodicity, etc. For this reason and also because it is sufficiently illustrative, it was preferable to study the LSM by simulation. It may, however, be interesting to know the behavior of the other parameters. Although problems of the mechanism can cause the machine velocity to deviate from the specified velocity, its experimental study can help to evaluate the algorithms presented here.

To perform experiments, the vehicle is situated over flat and horizontal terrain at a height of 350 mm. This is the base plane with respect to the body reference system that will be considered to perform adaptive-gait control. Instantaneous velocity has been obtained using the trajectory of a transmitter point on board the vehicle that has been registered using a 3D-dynamic localization system (Martín et al. 1993). The velocity values shown here have been obtained using registered positions, filtered previously using a median filter of 41 points and the corresponding temporal register. The number of samples required to calculate the median has been determined so that the velocity noise descends below the error of the measuring instrument (2 mm/s approximately). Instantaneous velocity is calculated using both position and time, and is filtered using the same procedure.

Figure 20 shows velocity as a function of time when the vehicle walks on stairs of 10 mm height and 50 mm depth. Peaks occur when a front leg lifts off. This is due to a sudden change in the position of the transmitter on board the vehicle. This phenomenon is related to flexion and backlash of the mechanisms that constitute the walking machine (Jiménez 1994). In this case, average velocity is given as 6.3 mm/s which approximates the commanded velocity, 6 mm/s. Fluctuations in velocity are due to the attitude and position-control method that modifies body velocity while a leg is in its transfer phase and while the four legs remain in the support phase, in order to maintain the desired trajectory of the vehicle.

Figure 21 shows the velocity when the vehicle walks up a slope of 12° and descends by the stairs described above. Peaks observed are produced when a front leg lifts off, as mentioned previously. Velocity is near 6 mm/s, but has fluctuations that can be explained by changes due to the attitude/position control method. At $t = 430$ s, the vehicle reaches the end of the slope and starts to go down the stairs. The average velocity is 6.7 mm/s. Velocity behavior is similar for the two types of terrain, as can be observed in the figure. It is convenient to remark that the measuring device is not appropriate for velocities this small. A device with an error of ± 2 mm/s must measure velocities of 200 mm/s to obtain errors of 1%.

9. Summary and Conclusions

This article presents an adaptive-gait control algorithm for periodic gaits. As a working example, a particular class of periodic gaits (called the wave-crab gait) and a quadruped robot were used. This strategy permits locomotion to be adapted to an irregular terrain in real time without the use of complex external sensors. It is very important to note that the theoretical wave-crab gait (and, in general, any other periodic gait with time restrictions) fails on very flat terrain (such as laboratory soil). However, the use of external perception sensors for this soil type appears unnecessary. Besides, this algorithm can be used by a walking vehicle with stereoceptive sensors when its information is very different from the real position of the soil. The objective of this strategy is to adapt the locomotion to the terrain while maintaining the wave gait, the body speed, and the static stability.

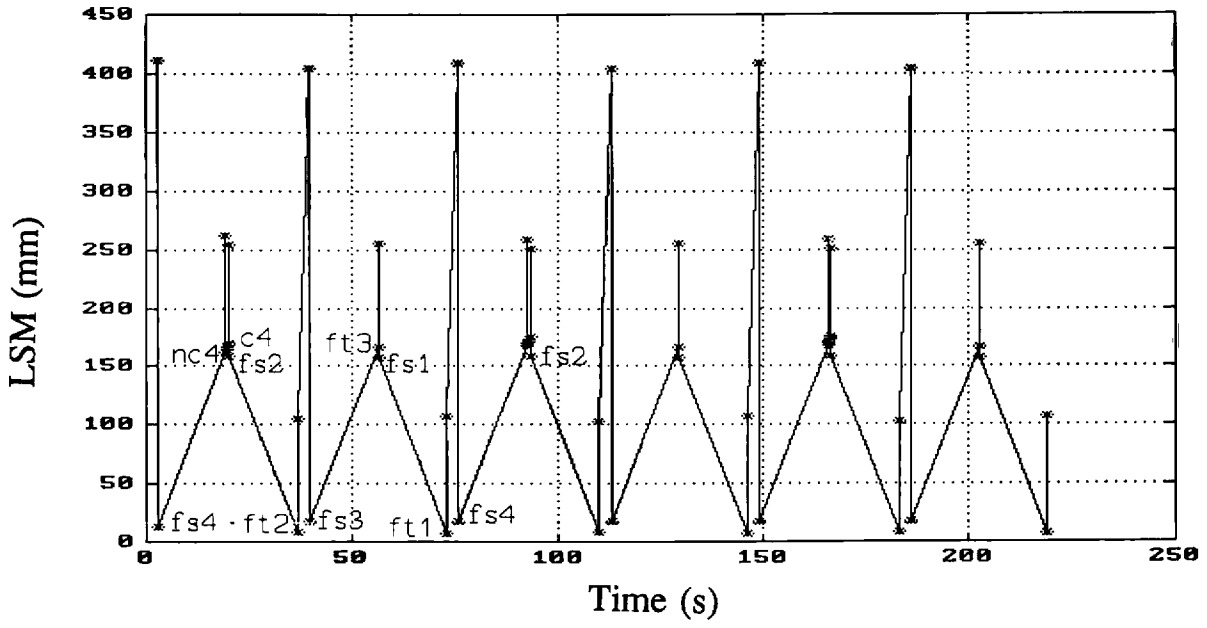

Fig. 18. Longitudinal stability margin for a wave gait with $\beta = 0.77$ and $\alpha = 0°$, and hollow and protrusion control.

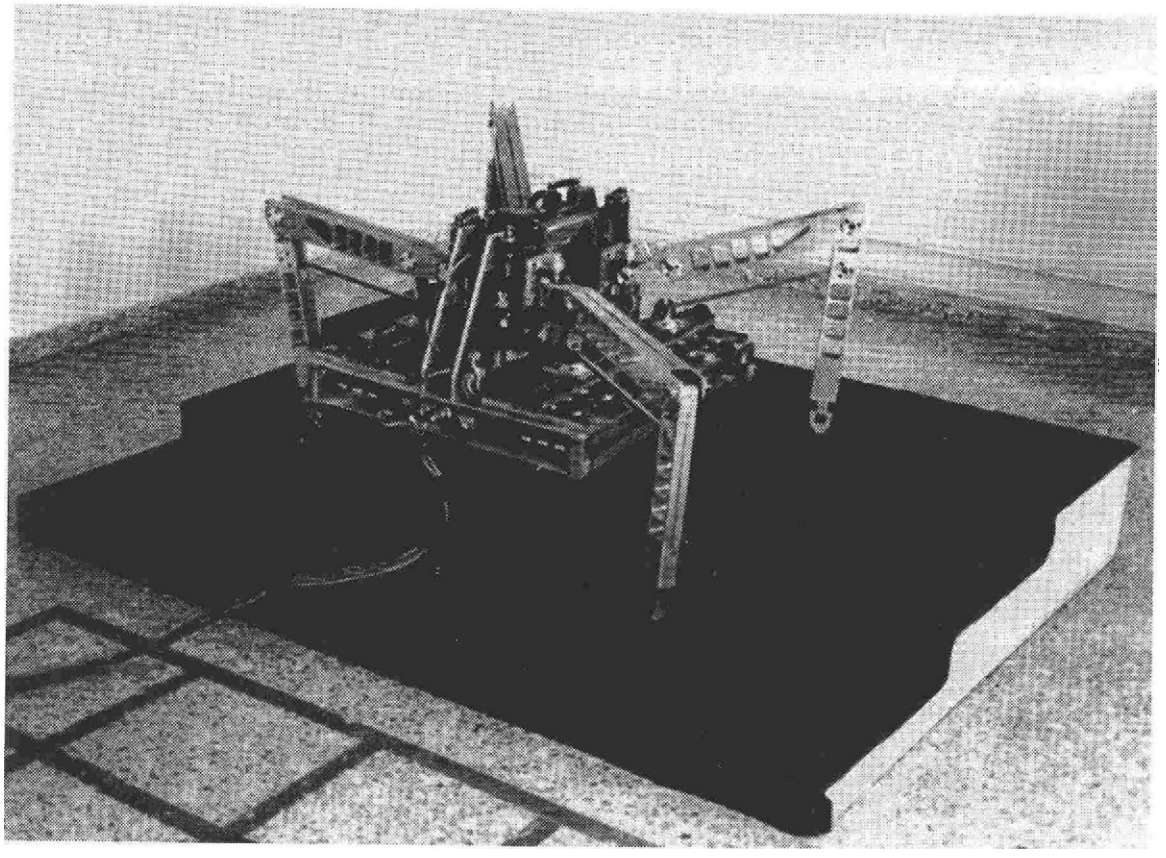

Fig. 19. The RIMHO walking machine.

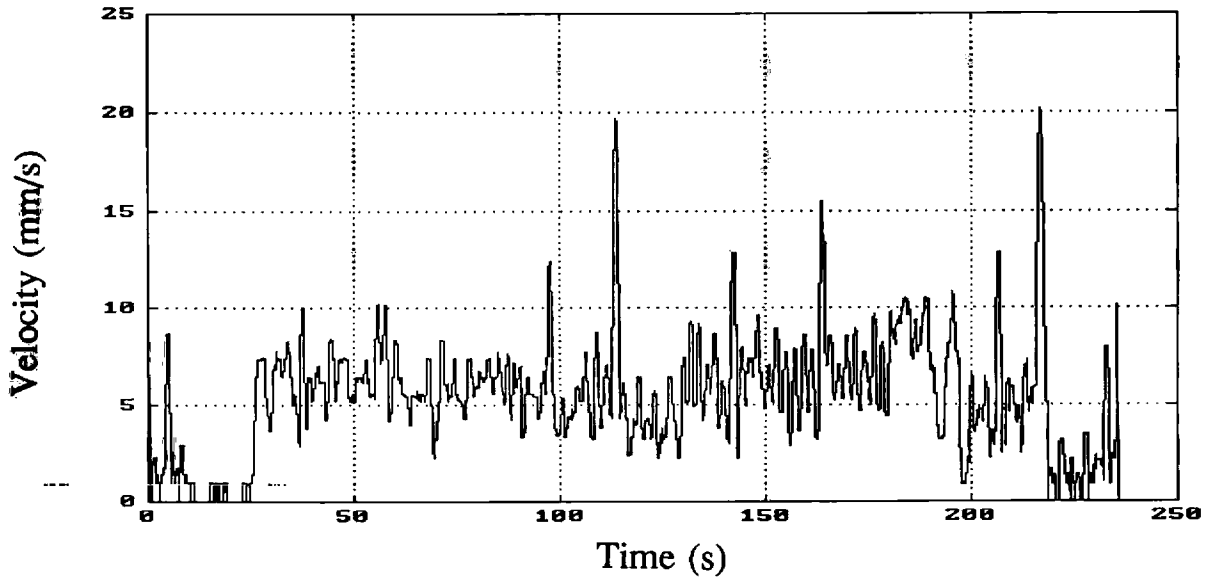

Fig. 20. Variation in velocity with time when the vehicle walks upstairs using the adaptive-gait algorithm.

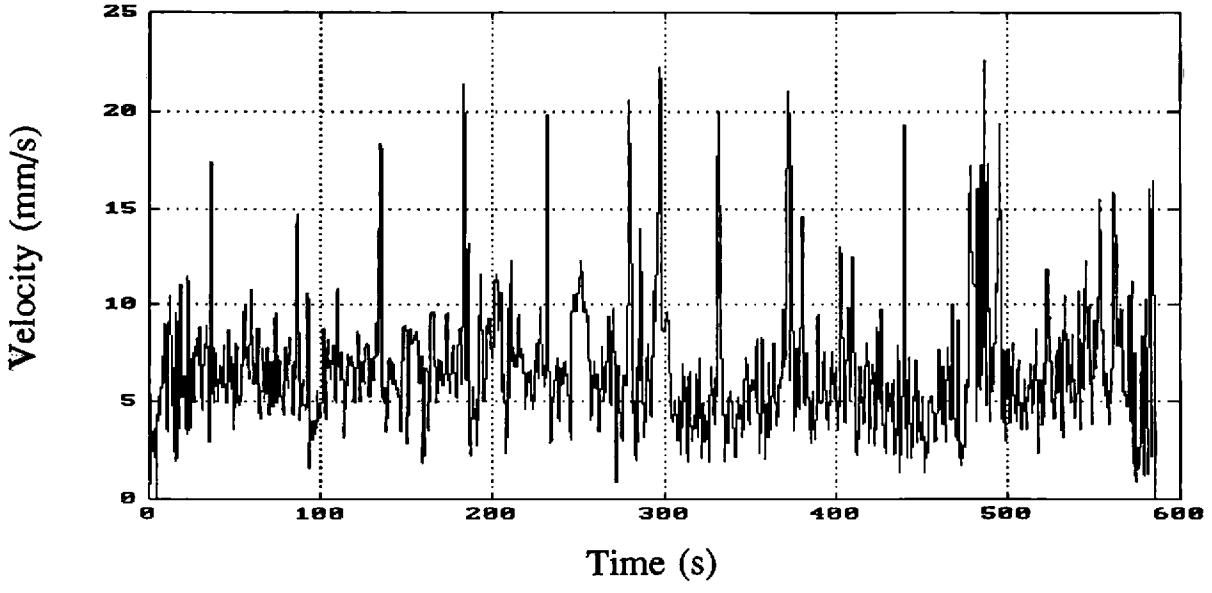

Fig. 21. Variation in velocity with time when the vehicle walks up a slope and then down some stairs using the adaptive-gait algorithm.

In this article, the irregular terrain has been characterized by a discrete model (*O*-type terrain), which results from combining the other two, which are called *OH*- and *OP*-types. Also, two methods of controlling gait parameters to adapt periodic locomotion to an irregular terrain have been defined: the stroke-control method and the velocity-control method. The adaptive-gait strategy to an *O*-type terrain has been described that treats the *OH*- and *OP*-types of adaptive gaits separately with good results. In the *OH*-type terrain-adaptive gait, the extra-transfer phase has been defined. Two types of extra-transfer trajectories (step and straight) have been studied in relation to stability, collision with the terrain, and attainable criteria; the straight trajectory was selected as the most suitable. Mathematical formulation of this strategy has been performed considering the increase of the stroke and the attainability of the leg that does not contact the ground. In the *OP*-type terrain-adaptive gait, the change in the leg stroke that places on a protrusion and its support trajectory have been formulated. Both strategies consider temporal restrictions natural for the periodic gait, the kinematic restrictions due to the constrained working volume and a measure of the static stability.

This adaptive-gait strategy has been incorporated into a computer control program together with other algorithms that permit the vehicle's attitude and altitude to be controlled. A number of simulations show how the longitudinal stability margin varies with the terrain. In addition, experimental results of the velocity behavior over steps and slopes maintaining body level been shown.

10. Acknowledgments

The authors would like to thank J. Tabera for his help in the implementation of the adaptive-gait control algorithm in the RIMHO walking machine, and J. Reviejo for his contributions in running the experiments. They also thank R. Ceres and his group for the design and implementation of the 3D position dynamic location system.

Support for this research has been provided by CICYT (Spain) under projects ROB90-1044-C02-01 and TAP94-0783.

References

Hirose, S. 1984. A study of design and control of a quadruped walking vehicle. *Int. J. Robot. Res.* 3(2):113–133.

Hirose, S., Iwasaki, H., and Umetani, Y. 1982. The basic study of the intelligence gait control of quadruped walking vehicles. *Trans. Soc. Instrument Control Eng.* 18(2):193–200.

Jiménez, M. A. 1994. Generation and implementation of wave gaits for quadruped robots. Ph.D. thesis, University of Cantabria, Department of Electronics.

Jiménez, M. A., González de Santos, P., and Armada, M. A. 1993 (April 18–21, University of Southhampton, Hampshire, UK). A four-legged walking test bed. In *Proceedings of the First IFAC International Workshop on Intelligence and Autonomous Vehicles.* D. Charnley, Pergamon Press, pp. 8–13.

Kumar, V. R., and Waldron, K. J. 1989. Adaptive gait control for a walking robot. *J. Robot. Sys.* 6(1):49–76.

Lee, W. J. 1984. A computer simulation study of omnidirectional supervisory control for rough-terrain locomotion by a multilegged robot vehicle. Ph.D. thesis, Ohio State University, Department of Electrical Engineering.

Lee, J. K., and Song, S. M. 1991. Path planning and gait of a walking machine in an obstacle-strewn environment. *J. Robot. Sys.* 8(6):801–827.

Martín, J. M., Ceres, R., Pérez, L. A., and Calderón, L. 1993. 3D-dynamic location system by ultrasonic techniques. Technical Report IAI-CSIC, Department of Systems.

Song, S. M., and Waldron, K. J. 1987. An analytical approach for gait study and its applications on wave gaits. *Int. J. Robot. Res.* 6(5):60–71.

Vargas, E., Jiménez, M. A., and Armada, M. A. 1991 (Dec. 11–12, Marseille). A graphic simulator for the telepresence station of a legged locomotion robot. *Proceedings of the 4th International Symposium on Offshore, Robotics and Artificial Intelligence.* pp. 152–162,

Zhang, C., and Song, S. M. 1990. Stability analysis of wave-crab gaits of a quadruped. *J. Robot. Sys.* 7(2):243–276.